# Enhancement and suppression effects of a nanopatterned surface on bacterial adhesion

Xinlei Li* and Tongsheng Chen

*MOE Key Laboratory of Laser Life Science and Institute of Laser Life Science, College of Biophotonics, South China Normal University, Guangzhou 510631, China*

(Received 31 January 2016; published 24 May 2016)

We present a quantitative thermodynamic model to elucidate the effects of a nanopatterned surface on bacterial adhesion. Based on the established model, we studied the equilibrium state of rodlike bacterial cells adhered to a nanopillar-patterned surface. Theoretical analyses showed the physical origin of bacterial adhesion on a nanopatterned surface is actually determined by the balance between adhesion energy and deformation energy of the cell membrane. We found that there are enhancement effects on bacterial adhesion to the patterned surface with large radius and small spacing of nanopillars, but suppression effects for nanopillars with a radius smaller than a critical value. In addition, according to our model, a phase diagram has been constructed which can clarify the interrelated effects of the radius and the spacing of nanopillars. The broad agreement with experimental observations implies that these studies would provide useful guidance to the design of nanopatterned surfaces for biomedical applications.

DOI: 10.1103/PhysRevE.93.052419

## I. INTRODUCTION

There is enormous interest in exploiting nanomaterials with nanoscale surface patterns in various biomedical applications because their size scale is similar to that of biological molecules (e.g., proteins and DNA) and structures (e.g., bacteria and viruses) [1–4]. The nanoscale surface patterns display remarkable surface properties, such as high hydrophobicity and strong biological activity on a cellular level due to their special topographical features with high aspect ratios [3,5]. Recent advances in nanobiotechnology and nanofabrication have stimulated novel applications in biomedicine where a nanopatterned surface is used to achieve self-cleaning, superhydrophobicity, and antibacterial activity [5–7].

In order to improve the effects of surfaces on their antibiofouling properties, i.e., the ability to eliminate or inhibit the extent of bacterial adhesion and biofilm formation, intensive efforts have been focused on the improvement of the performance of existing antibacterial surfaces, such as surface coating and surface chemical medication [3,8–12]. However, the surface coatings or medications have some significant drawbacks, e.g., the emergence of bacterial resistance against antibiotics or antibacterial agents, and diminished or absent antibacterial activity for a long time [12–14]. Recently, surfaces with nanopatterns that were inspired by the surface topographical features of insect wings were used to influence bacterial adhesion and even kill bacterial cells. For example, Ivanova *et al.* found that cicada wings with a nanopillar-patterned surface have a mechanical property for killing adherent bacterial cells such as some Gram-negative bacteria [15,16]. Then dragonfly wings with a similar patterned surface were found to kill Gram-positive bacteria as well as yeast [17,18]. Most recently, some artificial materials with similar nanopillars were also found to have bactericidal properties, such as black silicon, silicon, titania, titanium, and polymer [2,5,14,19–21]. Because the bactericidal properties of the nanopatterned surfaces are attributed to the mechanical rupture of the bacteria arising from physical interactions between the cells and the nanoscale surface structure, the method may be able to overcome drawbacks of the surface coatings or medications and have long-term antibacterial activity.

Despite the growing interest and considerable recent progress in the developing insect-inspired nanopatterned surfaces, the physical mechanisms of bactericidal effects are not well understood yet, and there is much to be learned about the specific mechanisms [16]. For example, what determines the degree of the bacterial adhesion on nanopatterned surfaces? How can bactericidal efficiency be improved by designing the surface topography of the nanopatterns? In order to attempt to design and fabricate new and preferable antibacterial surfaces, quantitative theories have been requested to study the effects of nanopatterned surfaces on bacterial adhesion.

Therefore, for this issue, in this paper we establish a quantitative thermodynamic model to elucidate the effects of a nanopatterned surface on bacterial adhesion. Our theoretical results reveal that the physical origin of bacterial adhesion on a nanopatterned surface is actually determined by the balance between adhesion energy and deformation energy of the cell membrane. We find that there are enhancement effects on bacterial adhesion to the patterned surface with large radius and small spacing of nanopillars, but suppression effects for the nanopillars with a radius smaller than a critical value. Furthermore, a phase diagram has been constructed which can clarify the interrelated effects of the radius and the spacing of nanopillars. We can identify from the phase the relation between the geometry of a nanopatterned surface and its bactericidal efficiency.

## II. THEORETICAL MODEL

Bacterial adhesion is a process that allows bacteria to attach or adhere to other organic and inorganic surfaces. When bacteria adhere to an inanimate surface, the adhesion reflects a specific interaction between the bacterial surface and the inorganic surface, in which the force of interaction is affected by the bacterial cell surface components and by the physiochemical properties of the materials. This adhesion process can

*xlli@scnu.edu.cn

 ©2016 American Physical Society

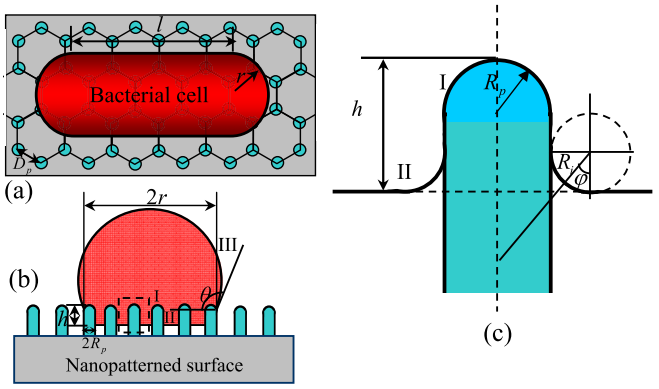


FIG. 1. (a) Schematic illustration of a rodlike bacterial cell adhered to a nanopatterned surface with nanopillars. (b) The cross section along the radius direction of bacterial cell. (c) The enlarged view of the membrane adhered to a nanopillar.

be described as the bacterial cell–surfaces interactions by an equilibrium thermodynamic model based on the assumptions that the time required for the deformation of the bacterial membrane is long enough to allow the equilibration between the adhered and unadhered membrane regions. Therefore, we can investigate the deformation conditions (including stretching degree) of the bacterial cell membrane to define the bactericidal properties of a nanopatterned substrate at the equilibration stage. In our model, further assumptions are that the bacterial cell membrane is a thin elastic layer and we neglect the thickness and composition of the layer [16]. Besides, the volume of a bacterial cell is considered to be constant during the bacterial adhesion process; i.e., the energy caused by the pressure difference between the outside and inside of the bacterial cell is neglected.

When a bacterial cell adheres to a nanopatterned surface, the bacterial cell membrane is partitioned into three regions, as shown in Fig. 1. The first is the free membrane regions on the top of the bacterial cell, the second is the contact adhesion region with the nanopatterned surface, and the third is the region immediately adjacent to the contact adhesion region. Apparently, the main change caused by bacterial adhesion includes two parts, the change of the cell membrane from free state to adhesion state and the deformation of the cell membrane. When the cell membrane changes from free state to adhesion state, energy can be released in chemical form. The deformation of the cell membrane results in the increase of energy as bending energy and stretching energy. Therefore, the free energy change caused by bacterial adhesion includes stretching energy, bending energy, and contact adhesion energy. Therefore the total free energy change of the bacterial cell on a nanopatterned surface can be written as

$$\Delta E = \frac{1}{2}\lambda\frac{\Delta S^2}{S_0} + \int_{S_{\text{cell}}}\left[\frac{\kappa}{2}(c_1+c_2-c_0)^2\right]dA - \int_{S_{ad}}\gamma dA - E_0^{\text{Bend}}, \quad (1)$$

where $\lambda$ is the stretching modulus of the membrane, $\Delta S$ and $S_0$ are the area change and initial total area of the bacterial cell membrane, $\kappa$ is the bending modulus of the membrane, $c_1$ and $c_2$ are two principal curvatures of the bending membrane surface, $c_0$ is the spontaneous curvature which is neglected in our model due to the large size of the cell, $\gamma$ is the contact adhesion energy density between the cell membrane and the surface, $S_{\text{cell}}$ and $S_{ad}$ are the total area and the adhesion area of the cell membrane, and $E_0^{\text{Bend}}$ is the deformed bending energy of the initial cell membrane. The first term is the stretching free energy penalty caused by deformation of the membrane; the second term represents the total bending energy of the cell membrane which can be calculated according to the Helfrich model [22,23]; the third term is the chemical energy release by the adhesion between the cell membrane and the nanopatterned surface, and the last term is the deformed bending energy of the initial cell membrane.

Equation (1) suggests that the total free energy is a function of the size of the deformed bacterial cell. Therefore, we can study the equilibrium state of the system during adhesion by minimizing the free energy function of Eq. (1). Taking the adhesion of a bacterial cell with a rodlike shape to a nanopatterned surface with cicada-wing-like structure as an example, we consider that the nanopatterned surface is covered by an array of nanopillars with a surface distribution density of $\xi$ (the number of nanopillars per unit area). Each nanopillar has a cylindrical shape with hemispherical caps with the radius of $R_p$, and the shape of the adhered bacterial cell is shown in Fig. 1. Because the deformed membrane of the cell is divided into three regions, the bending energy of the contact adhesion membrane in the second term of Eq. (1) is also divided into three parts: direct contact adhesion region (region I), the immediate region near the contact adhesion (region II), and the membrane at the top of the cell (region III). Therefore, we can write the total bending energy of the cell membrane as

$$\int_{S_{\text{cell}}}\left[\frac{\kappa}{2}(c_1+c_2-c_0)^2\right]dA = \int_{S_{\text{top}}+S_{ad}+S_{\text{imm}}}\left[\frac{\kappa}{2}(c_1+c_2-c_0)^2\right]dA, \quad (2)$$

where $S_{\text{top}}$, $S_{ad}$, and $S_{\text{imm}}$ are, respectively, the area of the top region, the contact adhesion region, and the region immediately near the contact adhesion. The area of the adhered bacterial cell can be calculated by $S_{\text{cell}} = S_{\text{top}} + S_{ad} + S_{\text{imm}}$. Considering the cross section of the bacterial cell has a spherical cap, the bending energy of the membrane at the top of the cell can be given by

$$\int_{S_{\text{top}}}\left[\frac{\kappa}{2}(c_1+c_2-c_0)^2\right]dA = \kappa\theta l/r + 4\pi\kappa(1-\cos\theta), \quad (3)$$

where $\theta$ is the contact angle of the bacterial cell with a patterned surface; $l$ and $r$ are the length and the width at the bottom of the contact interface with a patterned surface, as shown in Fig. 1.

Because the membrane adheres to the nanopillar-patterned surface, we assume that the adhered membrane has the same shape as the patterned surface. Therefore the bending energy of the membrane in the direct contact adhesion region can be

calculated as

$$\int_{S_{ad}} \left[\frac{\kappa}{2}(c_1+c_2-c_0)^2\right]dA = N_p[4\pi\kappa + \pi\kappa(h-R_p-R')/R_p], \tag{4}$$

where $h$ is the adhesion depth, $R'$ is the radius of region II, and $N_p = \xi(\pi r^2 + 2rl)$ is the total number of nanopillars under the bacterial cell.

The bending energy of the membrane in region II can be calculated by

$$\int_{S_{\text{imm}}} \left[\frac{\kappa}{2}(c_1+c_2-c_0)^2\right]dA = N_p \int_0^{\pi/2} \left\{\frac{\kappa}{2}\left[\frac{1}{R'} + \frac{\sin\varphi}{R_p+R'-R'\sin\varphi}\right]^2 2\pi[R_p+R'-R'\sin\varphi]R'\right\}d\varphi$$

$$= N_p\pi\kappa \int_0^{\pi/2} \frac{\left(\frac{R_p}{R'}+1\right)^2}{\left(\frac{R_p}{R'}+1\right)-\sin\varphi}d\varphi. \tag{5}$$

Because $(\frac{R_p}{R'}+1) > 1$, we have

$$\int_{S_{\text{imm}}} \left[\frac{\kappa}{2}(c_1+c_2-c_0)^2\right]dA = \frac{2N_p\pi\kappa\left(\frac{R_p}{R'}+1\right)^2}{\sqrt{\left(\frac{R_p}{R'}+1\right)^2-1}} \arctan\sqrt{\frac{\left(\frac{R_p}{R'}+1\right)+1}{\left(\frac{R_p}{R'}+1\right)-1}}. \tag{6}$$

According to Eq. (6), we can find that the bending energy of the membrane in region II is a function of $R_p/R'$. Therefore, we can obtain the equilibrium shape of the deformed membrane ($R_p$) by minimizing the bending energy. According to the values of Eq. (6) as a function of $R_p/R'$, we find that it has a minimum value of about $14.46\kappa$ when $R_p/R' \approx 0.599$; i.e.,

$$\int_{S_{\text{imm}}} \left[\frac{\kappa}{2}(c_1+c_2-c_0)^2\right]dA = 14.46N_p\kappa. \tag{7}$$

Therefore the total bending energy of the cell membrane can be calculated by

$$\int_{S_{\text{cell}}} \left[\frac{\kappa}{2}(c_1+c_2-c_0)^2\right]dA = \kappa\theta l/r + 4\pi\kappa(1-\cos\theta) + N_p[4\pi\kappa + \pi\kappa(h-R_p-R')/R_p] + 14.46N_p\kappa. \tag{8}$$

The stretching free energy in the first term of Eq. (1) can be known after calculating the change of the cell membrane area, $\Delta S = S - S_0$. The initial surface area of cell membrane, $S_0 = 4\pi R_0^2 + 2\pi R_0 l$, where $R_0$ is the initial radius of the cell. The adhered cell has the area of $S = S_{ad} + S_{\text{imm}} + S_{\text{top}}$ according to the foregoing. The total area of the adhesion region is $S_{ad} = N_p A_{ad}$, where $A_{ad} = 2\pi R_p^2 + 2\pi R_p(h - R_p - R')$ is the area of the contact adhesion region per nanopillar. The area of the top of the cell $S_{\text{top}} = 2r\theta l + 2\pi r^2(1-\cos\theta)$. The area of the membrane in region II can be calculated by

$$S_{\text{imm}} = N_p \int_0^{\pi/2} 2\pi[R_p+R'-R'\sin\varphi]R'd\varphi + (2\pi r + 2l)h + (\pi r^2 + 2rl) - \pi(R_p+R')^2 N_p;$$

that is,

$$S_{\text{imm}} = N_p[\pi^2 R'(R_p+R') - 2\pi R'^2] + (2\pi r + 2l)h + (\pi r^2 + 2rl) - \pi(R_p+R')^2 N_p,$$

where the first term is the area of the deformed membrane at the bottom of the cell, the second term represents the area of the outside edge of the bottom cell, and the last two terms are the area of the undeformed membrane in region II.

The dimensions of the adhered cell ($r$, $h$, and $\theta$) are associated with its volume. The sunken volume caused by the adhesion with a nanopillar is $V_{vs} = 2\pi R_p^3/3 + \pi R_p^2(h - R_p - R') + v_n$, where $v_n$ is the sunken volume in the deformed region II, and $v_n = \pi R'[\frac{2}{3}R'^2 - \frac{\pi}{2}R'(R_p+R') + (R_p+R')^2]$ according to $v_n = \int_0^{\pi/2} \pi[R_p+R'-R'\sin\varphi]^2 R'\sin\varphi d\varphi$. Therefore the total volume of the adhered cell can be given by $V = (2rl + \pi r^2)h + V_{\text{top}} - N_p V_{vs}$, where $V_{\text{top}} = 2\pi(r/\sin\theta)^2 l(1-\cos\theta) + \frac{1}{3}\pi(r/\sin\theta)^3(1-\cos\theta)^2(2+\cos\theta)$. According to the conservation of cell volume $V = V_0$, where $V_0 = 4\pi {R_0}^3/3 + \pi {R_0}^2 l$, we have the relation that

$$h = \frac{V_0 - \left\{V_{\text{top}} - N_p\left[2\pi R_p^3/3 + \pi R_p^2(-R_p - R') + v_n\right]\right\}}{2rl + \pi r^2 - N_p\pi R_p^2}. \tag{9}$$

Combining Eqs. (1)–(9), we can find that the total free energy change [Eq. (1)] of a bacterial cell adhered to a nanopatterned surface is a function of the dimensions of the adhered cell, $r$, $h$, and $\theta$. Because of the volume conservation of the bacterial cell, the total free energy change [Eq. (1)] is really just a function of two variables, $r$ and $\theta$, according to

the relation of Eq. (9). Therefore, we can find the equilibrium stage of the cell by minimizing the total free energy change as functions of $r$ and $\theta$.

### III. RESULTS AND DISCUSSION

The mechanical properties of the membrane of a bacterial cell have been investigated in some experiments and theory. The stretching modulus of bacterial membranes of *Escherichia coli* spheroplasts is about 0.5−2 mN/m; i.e., $\lambda \approx 0.12-0.5\ k_BT/\text{nm}^2$ [24]. Marsh reported that the bending modulus of a cell membrane with a monolayer structure is typically of the order of $10k_BT$ [25], and Cytrynbaum *et al.* estimated the bending modulus of a bacterial cell membrane to be $\kappa \approx 250-750$ pN nm [26]; i.e., $\kappa \approx 6-18k_BT$. Bacterial adhesion energy was predicted to be about 0−20 mJ/m$^2$; i.e., $\gamma \approx 0-0.5\ k_BT/\text{nm}^2$ [27]. Therefore, in our calculations, we used $\lambda = 0.25\ k_BT/\text{nm}^2$, $\kappa = 10k_BT$, and $\gamma = 0.2\ k_BT/\text{nm}^2$, respectively. Additionally, the radius and length of the rodlike bacterial cell are considered to be $R_0 = 200$ nm and $l = 2\ \mu$m. Figure 2(a) shows the calculated results of the total free energy change as a function of the bottom width ($2r$) at different contact angles $\theta$, 170°, 160°, 150°, 140°, 130°, and 120°, when the radius and spacing of the nanopillars are $R_p = 40$ nm and $D_p = 150$ nm, where the surface distribution density is $\xi = 2/(\sqrt{3}D_p^2)$. We can find that the free energy change has a minimum as a function of $r$ for a certain $\theta$, and the minima of the free energy change for different $\theta$ have the lowest value when $\theta$ is between 160° and 150°, as shown by the dashed line in Fig. 2(a). In order to search the lowest value of the free energy change, we calculated the minima of the free energy change as a function of $\theta$, as shown by Fig. 2(b). We find that the free energy change has the lowest value when $\theta \approx 155^\circ$ and $r \approx 75$ nm. In other words, the adhered bacterial cell is at the equilibrium stage in this case.

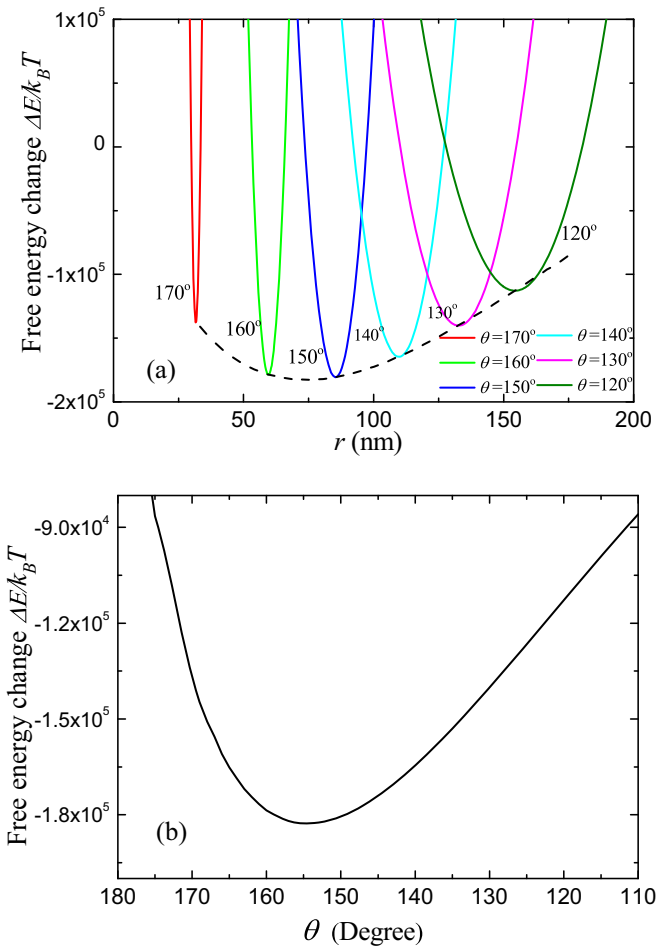


FIG. 2. (a) The calculated values of the total free energy change as a function of bottom width ($r$) at different contact angles $\theta$, from left to right, 170° (red), 160° (green), 150° (blue), 140° (cyan), 130° (magenta), and 120° (olive) when the radius and spacing of nanopillars are $R_p = 40$ nm and $D_p = 150$ nm. (b) The minima of the free energy change as a function of $\theta$.

Using the same method, we can analyze the effects of the size of nanopillars on the equilibrium stage of bacterial adhesion. Figure 3(a) shows the calculated results of the minima of free energy change as a function of $\theta$ for different radii of nanopillars (20, 30, 40, 50, and 60 nm) with the spacing of $D_p = 150$ nm, which indicate that the thick nanopillars have a high contact angle and a low free energy change at the equilibrium stage. When a bacterial cell is placed on a cicada-wing-like nanopatterned surface, the bacterial cell, such as *Pseudomonas aeruginosa*, has been known to be deformed and mechanically ruptured by the stretching from a nanopatterned surface [15,16]. Therefore, the bactericidal activity can be represented by the stretching degrees of the cell membrane. The larger the stretching degree is, the higher the bactericidal property is. Correspondingly, Fig. 3(b) shows the stretching degree of the cell membrane at the equilibrium stage which increases with increasing radius of the nanopillars. The larger stretching degree on the patterned surfaces with thick nanopillars means that more dead bacteria are obtained. The reason for the larger stretching degree on the patterned surfaces with thick nanopillars is that the adhesion to the patterned surface leads to a drastic increase of the contact adhesion area per unit of horizontal area, which is accompanied by increasing stretching strain of the membrane.

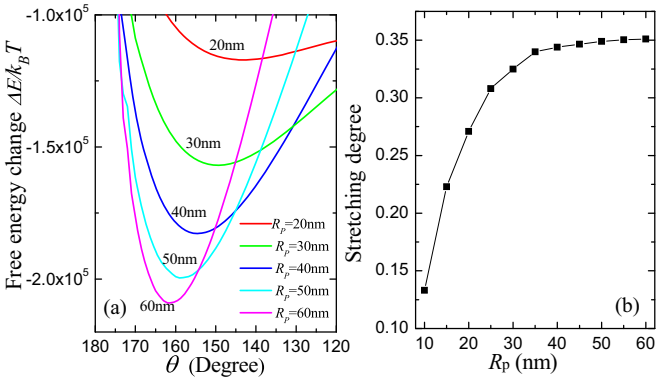


FIG. 3. (a) The calculated values of the minima of free energy change as a function of $\theta$ for different radii of nanopillars [from top to bottom, 20 nm (red), 30 nm (green), 40 nm (blue), 50 nm (cyan), and 60 nm (magenta)] with the spacing of $D_p = 150$ nm. (b) The calculated stretching degree of bacterial membrane at the equilibrium stage under different radii of nanopillars.

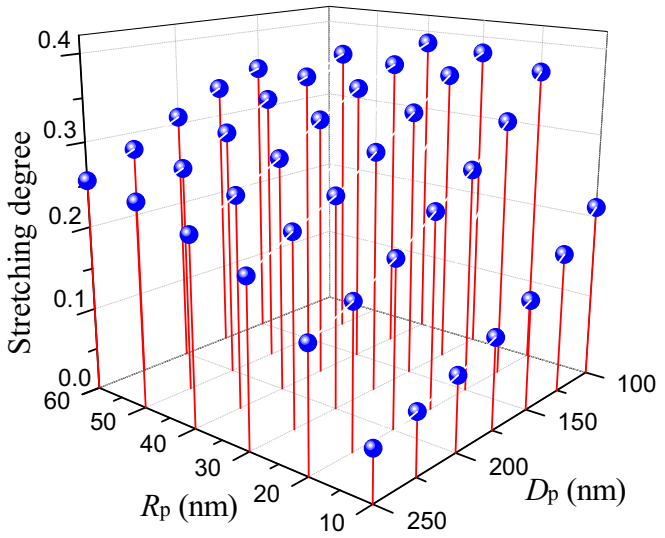


FIG. 4. The calculated stretching degree of bacterial membrane at the equilibrium stage under different radii and spacing of nanopillars.

Besides the effects of the radius of the nanopillars, the increase of the spacing between nanopillars can also result in the increase of the contact adhesion area per unit of horizontal area. Therefore, the spacing between nanopillars should also play an important role in the bactericidal property. Figure 4 shows the calculated stretching degree for different $R_p$ and $D_p$ of nanopillars. We can find that larger $R_p$ and smaller $D_p$ lead to greater stretching degrees, which is caused by the increase of the contact adhesion area per unit of horizontal area to surface. Theoretical results indicate that bactericidal efficiency can be enhanced by properly increasing the surface distribution density and radius of nanopillars.

The theoretical analyses above show that the physical origin of the effects of a patterned surface on bacterial adhesion is actually determined by the balance between adhesion energy and deformation energy including bending energy and stretching energy of the membrane. When a bacterial cell attaches to the patterned surface, the adhesion will occur. During the process, the deformation energy caused by nanopillars limits the bacterial adhesion. When the adhesion energy is smaller than the deformation energy, further bacterial adhesion is terminated. Correspondingly, for the effects of a patterned surface on bacterial adhesion, the bacterial adhesion is actually influenced by the competition between the surface roughness and the thickness of the nanopillars, where we define surface roughness as the deviations of the real surface area from its area of ideal smooth surface. The patterned surface with high roughness, i.e., with large radius and small spacing of nanopillars, provides more exposed regions for adhesion. Therefore, the patterned surface with large radius and small spacing of nanopillars has strong properties for bacterial adhesion and high stretching degree of the cell membrane. In detail, the nanopillars with a large radius correspond to a high stretching degree when the spacing of the nanopillars is fixed, and the nanopillars with small spacing also correspond to a high stretching degree when the radius of the nanopillars is fixed, as shown in Fig. 4. On the other hand, nanopillars cause the increase of the deformation of the membrane, which limits the bacterial adhesion to the surface. The thin nanopillars provide strong resistance due to their large surface curvature, so the patterned surface with a small nanopillar radius has weak properties for bacterial adhesion. At the critical condition, the bacterial cell cannot adhere to the patterned surface when the radius of nanopillars is smaller than a certain value. According to Eq. (1), we can calculate the critical radius of nanopillars for bacterial adhesion through comparing the bending energy with adhesion energy.

The bending energy of a membrane caused by adhesion to a nanopillar can be given by $E_p^{\mathrm{Bend}} = 4\pi\kappa + \pi\kappa(h - R_p - R')/R_p + 14.46\kappa$ based on Eqs. (4) and (7). The adhesion energy per nanopillar is $E_p^{Ad} = \gamma[2\pi {R_p}^2 + 2\pi R_p(h - R_p - R')]$. Only if the adhesion energy is larger than the bending energy, i.e., $E_p^{Ad} > E_p^{\mathrm{Bend}}$, can the bacterial cell proceed to adhesion. Considering that $h \gg (R_p + R')$, according to $E_p^{\mathrm{Bend}} = E_p^{Ad}$, we can obtain the critical radius of nanopillars for bacterial adhesion as

$$R_p^* = \sqrt{\kappa/2\gamma}. \tag{10}$$

Equation (10) means that the bending energy is always larger than the adhesion energy when the radius of nanopillars is smaller than $\sqrt{\kappa/2\gamma}$. Therefore, it is impossible for the bacterial cell to adhere to such a nanopatterned surface when $R_p < \sqrt{\kappa/2\gamma}$. In this case, combining the calculated results of the stretching degree of the membrane as functions of the size of the nanopatterned surface, we can construct a phase diagram of the bactericidal activity on the $R_p - D_p$ (radius versus spacing of nanopillars) plane, as shown in Fig. 5. According to Fig. 5, we can find that the large radius and small spacing lead to the stretching degree increase, and contrarily the small radius and large spacing result in the stretching degree decrease. A high value of stretching degree

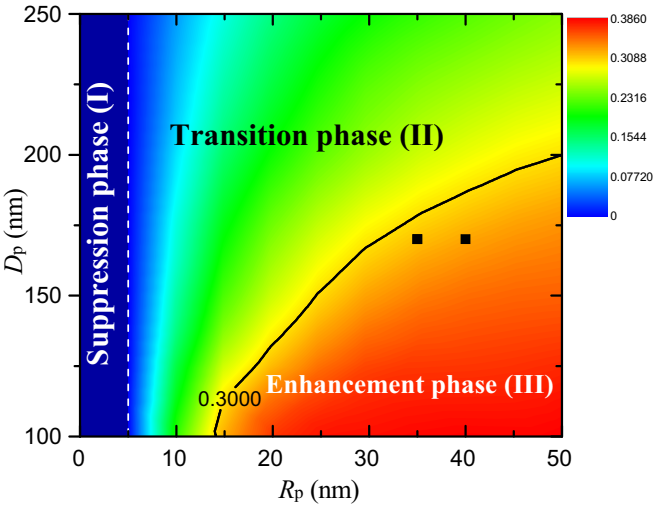


FIG. 5. The phase diagram of the bactericidal activity in the space of $R_p - D_p$ (radius versus spacing of nanopillars). The color bar indicates the values of stretching degree of bacterial membrane [the red indicates high value (enhancement phase), and blue indicates low value (suppression phase)]. The white dashed line is the critical radius for bacterial adhesion based on Eq. (11). The squares represent the experimental results [15,19].

corresponds to strong bactericidal activity, while a low value of stretching degree corresponds to weak bactericidal activity. On the other hand, when the radius of the nanopillars is smaller than $\sqrt{\kappa/2\gamma}$, it is impossible for a bacterial cell to adhere (stretching degree is zero). Thus, in the phase diagram, three characteristic regions separated by two phase transition boundaries (white and black lines) can be identified. Region I shows that bactericidal activity vanishes, and is therefore noted as the "suppression phase." In both regions II and III, bacterial adhesion appears; we denote these two regions, respectively, as "transition phase" and "enhancement phase," according to the values of stretching degree. The lower transition boundary follows well with the size limit (white line) set by Eq. (10). The higher transition boundary (black line) is set for the value of stretching degree of 30%. In the phase diagram of bactericidal activity, one can note that the bactericidal activity is noticeably higher for the large radius and small spacing of nanopillars. Theoretical results indicate that bactericidal activity can be enhanced by increasing surface roughness, i.e., increasing the surface distribution density and radius. These results agree well with the experimental reports [15,16]. The surface of the wings of the cicada *Psaltoda claripennis* is covered with a periodic topography consisting of hexagonal arrays of spherically capped, conical, nanoscale pillars, and the spacing and radius of the nanopillars are 50 nm in radius at the base, 30 nm in radius at the cap, and spaced 170 nm apart from center to center. The cicada-wing nanopillars are extremely effective at killing *Pseudomonas aeruginosa* cells based solely on their physical surface structure. In addition, Dickson *et al.* find that the percentage of dead cells increases by 16% on nanopillared surfaces with the spacing of 380 nm, while a 97% increase is measured on the surfaces with the spacing of 130 nm, and a 114% increase is measured on the surfaces with the spacing of 100 nm compared with that on the flat surface, which shows that more closely spaced nanopillars, i.e., the larger surface distribution density of nanopillars, are more effective at killing bacterial cells [19]. These experimental observations suggest that the bactericidal properties can be strongly influenced by the surface topology and agree well with our modeling results.

Noticeably, in our model, we consider that the adhered bacterial cell is rod shaped, for example, *Escherichia coli*. In fact, there are also many bacterial cells with a spherical shape, including cocci, such as *Staphylococcus aureus*. Although we take a rodlike bacterial cell as an example, our model can be used for the bacterial cells with a spherical shape. In our model, we consider that the rodlike bacterial cell has a cylindrical shape with hemispherical caps at two ends, in which the length of the cylindrical part is $l$ and the radius of the hemispherical cap is $R_0$, as shown in Fig. 1. If we set $l = 0$, the shape of the bacterial cell becomes a spherical shape with the radius of $R_0$. In other words, our model can be used to investigate the adhesion of the spherical bacterial cells when $l = 0$. In addition, we assume that the nanopatterned surface can bind with the bacterial cell, reducing its motility, including for swimming and swarming. Though some bacterial cells including *Escherichia coli* are highly motile, the cells can fasten to the nanopillared surface once they attach to the patterned surface due to the strong adhesion energy caused by the drastic increase of the contact area. Experimental observations have shown that there is no obvious phenomenon of accumulation and the bacterial cell can adhere separately to a nanopatterned surface [15,19]. On the other hand, the high-motility bacterial cells usually are easy to deform, i.e., have low bending and stretching modulus. In this case, the deformation energy caused by the nanopatterned surface becomes weak and less resistant according to our model [Eq. (8) has shown that the bending energy is proportional to the bending modulus]. Therefore, the high-motility bacteria are less resistant to nanopatterned surfaces. The results are consistent with experimental observations, in which Gram-positive bacteria with greater rigidity were observed to remain viable and be unaffected by the nanopillar structures. However, by decreasing the rigidity of surface-resistant strains through microwave irradiation, these cells become sensitive to the bactericidal mechanisms of the nanopillar structures [15,16].

## IV. CONCLUSION

In summary, in order to gain a better understanding of the effects of nanopatterned surface on bacterial adhesion, we have proposed a quantitative thermodynamic model to elucidate the mechanism of the bacterial adhesion to the nanopatterned surface. Our theoretical results reveal that the physical origin of the bacterial adhesion to a nanopatterned surface is actually determined by the balance between adhesion energy and deformation energy of the cell membrane. We found that the adhesion energy can be enhanced due to the drastic increase of the contact adhesion area caused by the large surface roughness, but deformation energy can also be increased, caused by nanopillars with a small radius. According to the calculated results, we obtained a phase diagram of the bacterial adhesion to the nanopatterned surface, which can clarify the interrelated effects of the radius and the spacing of nanopillars. Our theoretical results seem to show broad agreement with experimental observations, which implies that these studies would provide useful guidance to the design of nanopatterned surfaces for antibacterial applications.

## ACKNOWLEDGMENTS

This work was financially supported by National Natural Science Foundation of China (Grants No. 61527825, No. 81471699, and No. 11104084), the Guangdong Province Science and Technology Plan Project (Grant No. 2014B090901060).

[1] D.-H. Kim, H. Lee, Y. K. Lee, J.-M. Nam, and A. Levchenko, Adv. Mater. **22**, 4551 (2010).

[2] T. Diu, N. Faruqui, T. Sjöström, B. Lamarre, H. F. Jenkinson, B. Su, and M. G. Ryadnov, Sci. Rep. **4**, 7122 (2014).

[3] E. K. F. Yim, R. M. Reano, S. W. Pang, A. F. Yee, C. S. Chen, and K. W. Leong, Biomaterials **26**, 5405 (2005).

[4] A. Mahdavi *et al.*, Proc. Natl. Acad. Sci. U. S. A. **105**, 2307 (2008).

[5] E. P. Ivanova, J. Hasan, H. K. Webb, G. Gervinskas, S. Juodkazis, V. K. Truong, A. H. F. Wu, R. N. Lamb, V. A. Baulin, G. S. Watson, J. A. Watson, D. E. Mainwaring, and R. J. Crawford, Nat. Commun. **4**, 2838 (2013).
[6] T. Darmanin and F. Guittard, Mater. Today **18**, 273 (2015).
[7] B. Bhushan and Y. C. Jung, Prog. Mater. Sci. **56**, 1 (2011).
[8] I. Banerjee, R. C. Pangule, and R. S. Kane, Adv. Mater. **23**, 690 (2011).
[9] I. C. Saldarriaga Fernández, H. C. van der Mei, M. J. Lochhead, D. W. Grainger, and H. J. Busscher, Biomaterials **28**, 4105 (2007).
[10] D. Davies, Nat. Rev. Drug Discovery. **2**, 114 (2003).
[11] C. Chang, X. Huang, Y. Liu, L. Bai, X. Yang, R. Hang, B. Tang, and P. K. Chu, Electrochim. Acta **173**, 345 (2015).
[12] J. Hasan, H. Webb, V. Truong, S. Pogodin, V. Baulin, G. Watson, J. Watson, R. Crawford, and E. Ivanova, Appl. Microbiol. Biotechnol. **97**, 9257 (2013).
[13] A. Bridier, R. Briandet, V. Thomas, and F. Dubois-Brissonnet, Biofouling **27**, 1017 (2011).
[14] J. Hasan, S. Raj, L. Yadav, and K. Chatterjee, RSC Adv. **5**, 44953 (2015).
[15] E. P. Ivanova, J. Hasan, H. K.Webb, V. K. Truong, G. S. Watson, J. A. Watson, V. A. Baulin, S. Pogodin, J. Y. Wang, M. J. Tobin, C. Löbbe, and R. J. Crawford, Small **8**, 2489 (2012).
[16] S. Pogodin, J. Hasan, V. A. Baulin, H. K. Webb, V. K. Truong, T. H. P. Nguyen, V. Boshkovikj, C. J. Fluke, G. S. Watson, J. A. Watson, R. J. Crawford, and E. P. Ivanova, Biophys. J. **104**, 835 (2013).
[17] E. P. Ivanova, S. H. Nguyen, H. K. Webb, J. Hasan, V. K. Truong, R. N. Lamb, X. Duan, M. J. Tobin, P. J. Mahon, and R. J. Crawford, PLoS ONE **8**, e67893 (2013).
[18] K. Nowlin, A. Boseman, A. Covell, and D. LaJeunesse, J. R. Soc., Interface **12**, 20140999 (2014).
[19] M. N. Dickson, E. I. Liang, L. A. Rodriguez, N. Vollereaux, and A. F. Yee, Biointerphases **10**, 021010 (2015).
[20] C. Serrano, L. García-Fernández, J. P. Fernández-Blázquez, M. Barbeck, S. Ghanaati, R. Unger, J. Kirkpatrick, E. Arzt, L. Funk, P. Turón, and A. del Campo, Biomaterials **52**, 291 (2015).
[21] S. Christina, L. Michael, M. Yahya, B. Anna, K. Chinmay, S. B. Pio John, A. S. Thomas, L. Alfred, and K. Manfred, Nanotechnology **25**, 195101 (2014).
[22] P. B. Canham, J. Theor. Biol. **26**, 61 (1970).
[23] W. Helfrich, Z. Naturforsch., C: Biochem., Biophys., Biol., Virol. **28**, 693 (1973).
[24] Y. Sun, T.-L. Sun, and H. W. Huang, Biophys. J. **107**, 2082 (2014).
[25] D. Marsh, Chem. Phys. Lipids **144**, 146 (2006).
[26] E. N. Cytrynbaum, Y. D. Li, J. F. Allard, and H. Mehrabian, Phys. Rev. E **85**, 011902 (2012).
[27] X. Zhang, Q. Zhang, T. Yan, Z. Jiang, X. Zhang, and Y. Y. Zuo, Environ. Sci. Technol. **49**, 6164 (2015).